Interfacial Behavior of Anionically Synthesized Amphiphilic Star Block Copolymers Based on Polybutadiene and Poly(ethylene oxide) at the Air/Water Interface

Rachid Matmour,[†,‡] Raju Francis,[‡,§] Randolph S. Duran,[*,‡] and Yves Gnanou[*,†]

Laboratoire de Chimie des Polymères Organiques (LCPO), ENSCPB−CNRS-Université Bordeaux 1, 16 Avenue Pey-Berland, 33607 Pessac Cedex, France, and The George and Josephine Butler Polymer Research Laboratory, Department of Chemistry, University of Florida, P.O. Box 117200, Gainesville, Florida 32611-7200

Received March 18, 2005; Revised Manuscript Received June 21, 2005

ABSTRACT: We describe the preparation and the surface properties of monolayers of a new set of (PB-*b*-PEO)$_4$ amphiphilic four-arm star block copolymers. A divergent anionic polymerization method yielded copolymers with well-defined molecular weights, block volume fractions, and architecture. Initially, tri- and tetracarbanionic initiators were used to initiate the polymerization of butadiene followed by end-capping of living chains with ethylene oxide. The tri- and tetrafunctionalities of the resulting hydroxyl-terminated star polydienes were confirmed by ^{1}H NMR spectroscopy. The four-arm star polymeric alcohols were then titrated with diphenylmethylpotassium to yield the analogous potassium alkoxides. The resulting macroinitiators were used to polymerize corona blocks of ethylene oxide. Different samples of well-defined (PB-*b*-PEO)$_4$ amphiphilic star block copolymers exhibiting narrow molar mass distribution were prepared with poly(ethylene oxide) over a range of volume fractions. Isotherm experiments at the air/water interface showed the following three characteristic regions: a compact brush region, a pseudoplateau at a pressure of ca. 10 mN/m, and a pancake region where the observed surface area depended on the amount of PEO present. The elasticity properties of the monolayer were examined by repetative compression/expansion cycles and resulted in reproducible hysteresis at different pressures. The monolayers were also transferred as Langmuir−Blodgett films on mica at various surface pressures and analyzed by atomic force microscopy (AFM), demonstrating different morphologies from analogous (PS-*b*-PEO)$_4$ star copolymers.

1. Introduction

Amphiphilic block copolymers containing both hydrophilic and hydrophobic segments form an important class of materials due to their wide variety of potential applications as polysoaps, polymeric surfactants, solution modifiers, emulsifiers, wetting agents, foam stabilizers, and drug carriers.[1−3] In most of the above areas, controlling the size as well as the surface properties of block copolymer assemblies is a major issue. In this study, we investigate star copolymers containing poly(butadiene) (PB) blocks.

The amphiphilic character of block copolymers has also been widely exploited for the preparation of monolayers at the air/water interface. These monolayers are somewhat different from classical low molecular weight amphiphiles in that the copolymer is constituted of hydrophilic and hydrophobic blocks of considerable molecular weight. The hydrophilic block by itself would be soluble in water, but the hydrophobic block acts as a buoy, anchors the polymer chains at the interface, and thus prevents the hydrophilic part from dispersing into the bulk water subphase. Numerous studies published on the field of monolayers at the air/water interface during the past years demonstrate the utility in using the nonelectrolyte poly(ethylene oxide) (PEO) water-soluble block due in particular to its properties and its biocompatibility and subsequent potential for applications in drug-delivery and other fields.[4,5] Among copolymers investigated at the air/water interface, the polystyrene-*block*-poly(ethylene oxide) (PS-*b*-PEO) block copolymers certainly form the most commonly studied systems.[6−18]

Although PS is a convenient choice due to its inexpensive price, monomer availability, and facile synthesis, polybutadiene-*b*-poly(ethylene oxide) (PB-*b*-PEO) is the primary amphiphilic diblock copolymer studied to provide control over spherical rodlike and vesicular architectures in bulk or aqueous solutions.[19−22] Furthermore, polybutadiene offers the possibility to stabilize block copolymer assemblies by cross-linking through the pendant double bond of the 1,2-polybutadiene units. This emerging approach to bridging the nanoscale world of labile, interfacially driven self-assemblies with the meso-scale has resulted in several examples of massively cross-linked 3D structures.[22−25] In the case of PB-*b*-PEO diblock copolymers, Bates et al. are the first group to succeed to retain the cylindrical morphology formed by gigantic wormlike rubber micelles of PB-*b*-PEO copolymers in water by chemically cross-linking of the PB cores.[22,26]

However, despite the significant interest showed for PB-*b*-PEO copolymers, few groups have studied the behavior of such amphiphiplic copolymers at the air/water interface.[27−29] Among these, only Discher et al. were able to show characteristic morphological organization of this amphiphile at the air/water interface through AFM images and were the only ones who attempted cross-linking stabilization.[27] Moreover, the behavior of any PB-*b*-PEO diblock copolymer with architecture more complex than linear chains, whether

[†] ENSCPB−CNRS−Université Bordeaux 1.
[‡] University of Florida.
[§] Permanent address: Department of Chemistry, St. Joseph's College, Devagiri (University of Calicut), Calicut, Kerala, India.
* To whom all correspondence should be addressed: e-mail duran@chem.ufl.edu, Fax 352-392-9741; e-mail gnanou@enscpb.fr, Fax 33 (0)5 40 00 84 87.

10.1021/ma050578z CCC: $30.25
Published on Web 08/09/2005

Scheme 1. (PB-*b*-PEO)$_4$ Four-Arm Amphiphilic Star Block Copolymers

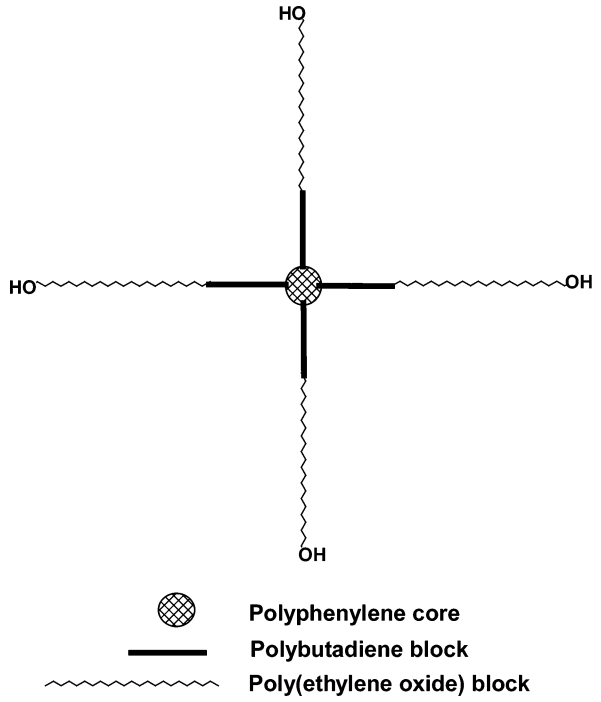

in bulk, in solution, or at the interface, has not yet been investigated.

The structure of the AB diblock copolymers either in the bulk state or in solution is most certainly influenced by the volume fraction of each block and by the segment−segment interaction parameter χ, but the molecular architecture, the conformational asymmetry, and the compositional fluctuations all also have an effect on structure.[30] Systematic investigation of the influence of all these factors on the organization of AB diblock copolymers in a star architecture necessitates the preparation of monodispersed materials with well-defined molecular weights, block volume fractions, and architecture.[31]

In this paper, we present the first synthesis of (PB-*b*-PEO)$_4$ amphiphilic star block copolymers based on a polybutadiene core and poly(ethylene oxide) corona by anionic polymerization (Scheme 1). The divergent or "core-first" method appears to be the best route to prepare such materials. The convergent method would require the synthesis first of PEO-*b*-PB$^-$Li$^+$ linear living chains with a first block of PEO and a second block of PB, which is not known to date. The only attempt to synthesize PB-*b*-PEO block copolymer with complex architecture was the work of Xu et al.,[32] who prepared 12-arm PB-*b*-PEO heteroarm or miktoarm star copolymers by coupling of V-shaped PB-*b*-PEO chains to an aryl ester dendrimer core; these were certainly not star block copolymers containing PEO blocks at the corona and PB blocks at the core as in our case so that both bulk and solution properties would be different. Moreover, anionic polymerization in general suffers from lack of pluricarbanionic initiators exhibiting precise functionality and good solubility. Consequently, while significant success in controlled radical and cationic polymerization of multiarmed species has been described, to date only three attempts have been successful in the area of pluricarbanionic initiators.[33−35] In a previous study, we presented the synthesis of novel tri- and tetracarbanionic initiators based on a halogen−lithium exchange reaction and the first example of well-defined three- and four-arm polystyrene and polybutadiene stars obtained by the "core-first" method.[36]

As a hydrophobic block, PB should provide a material well-above its glass transition and therefore highly fluid at ambient temperatures. In this work, the synthesis, surface behavior of the four-arm star amphiphilic copolymer, (PB-*b*-PEO)$_4$, at the air/water interface, and initial AFM images of transferred monolayer films on mica are discussed. The surface behavior of this homologous series is also compared to PS-*b*-PEO, the most extensively studied nonelectrolyte copolymer system.

2. Experimental Section

Materials. Benzene for polymerizations was dried and distilled twice over CaH_2 and polystyryllithium successively. THF was purified by distillation over CaH_2 and then from a purple Na/benzophenone solution. 2-Methoxyethanol (Aldrich, 99%) was magnesium-dried and distilled. Solutions of *sec*-butyllithium (*s*-BuLi) (Aldrich) were used for halogen−lithium exchange reaction after double titration.[37] The diphenylmethylpotassium (DPMK) solution was prepared and titrated following procedures described elsewhere.[38] Butadiene (B) (Aldrich, 99%) was stirred over *sec*-BuLi at −30 °C for 2 h and distilled prior to use. Ethylene oxide (EO) (Fluka, 99.8%) was stirred over sodium for 3 h at −40 °C and then distilled before use. For the synthesis of the tri- and tetrabromoinitiators, we followed the procedures described by Cheng et al.[39] and Wolfe et al.,[40] respectively.

Instrumentation. High-purity argon (>99.5%) was rigorously dried and deoxygenated by passage through a column containing vermiculite. ^{1}H NMR spectra were recorded on a Bruker AC400 spectrometer using $CDCl_3$, CD_2Cl_2, and CD_3-OD as deuterated solvents. Chemical shifts are reported in ppm (δ) downfield from tetramethylsilane (TMS) and referenced to residual protio solvent. Apparent molar masses were determined with a size exclusion chromatography (SEC) equipped with four TSK-gel columns (7.8 × 30 cm, 5 μm, G 2000, 3000, 4000, and 5000 HR with pore sizes of 250, 1500, 10 000, and 100 000 Å, respectively) and THF as the mobile phase (1 mL/min). This instrument was equipped with a refractive index (RI) (Varian RI-4) and UV−vis (Varian 2550 variable λ) detectors. The SEC was calibrated using linear polystyrene samples. Absolute molar masses of (PB-OH)$_4$ stars were calculated using a multiangle laser light scattering (MALLS) detector (DLS) (Wyatt Technology) connected to an SEC line (abbreviated SEC/DLS in the following). The dn/dc values for (PB-OH)$_4$ stars were measured in THF at 25 °C with a laser source (dn/dc = 0.094 cm^3/g). The tetrabromo initiator was characterized by mass spectrometry and elemental analysis.

Langmuir Films. Surface film characterization was accomplished using a Teflon Langmuir trough system (KSV Ltd., Finland) equipped with two moving barriers and a Wilhelmy plate for measuring surface pressure. Isotherm and hysteresis experiments were performed at least three times to verify reproducibility. Between runs, the trough was cleaned with ethanol and rinsed several times with Millipore filtered water of ~18 MΩ cm^{-1} resistivity. Samples were typically prepared by dissolving ~1 mg of copolymer in 1 mL of chloroform and spread dropwise with a gas-tight Hamilton syringe on the Millipore water subphase. The chloroform was then allowed to evaporate for 30 min to ensure no residual solvent remained. The subphase temperature was maintained at 25 °C through water circulating under the trough. Both isotherm and hysteresis experiments were run with barrier movement not exceeding 10 mm min^{-1}. Compression for isotherms occurred in a linear fashion at a rate of 0.4 mN/(m min). The compression/expansion cycles for the hysteresis experiments were repeated five times after a delay of 30 min, during which the monolayer was allowed to relax at Π = 0 mN m^{-1}. The data resulting from the isotherms (A_0, ΔA, and A_{pancake}) were plotted vs the number of EO units and fitted by a linear curve.

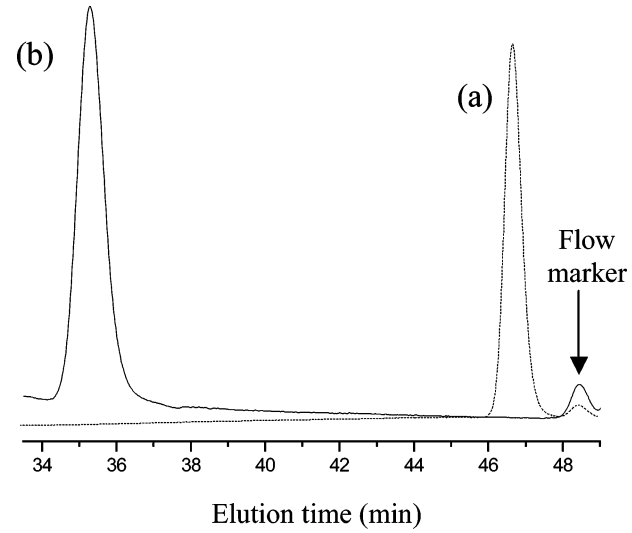

Figure 1. Size exclusion chromatography trace of the tetrabromoinitiator (a) and of the $(PB\text{-}OH)_4$ hydroxyl ended star polymer (b) in THF ($M_{w,DLS}$ = 16 400 g mol^{-1}; M_w/M_n = 1.05).

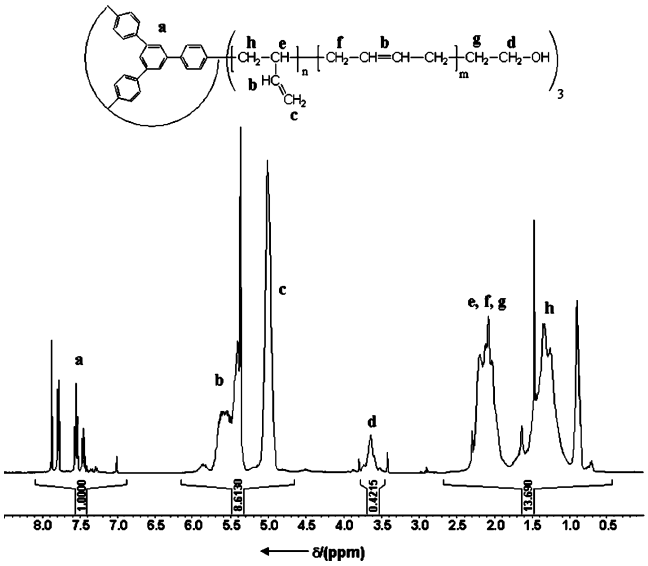

Figure 2. ^{1}H NMR spectra (CD_2Cl_2, 400 MHz) of $(PB\text{-}OH)_3$ hydroxyl ended star polymers ($M_{w,DLS}$ = 2400 g mol^{-1}; M_w/M_n = 1.1).

Atomic Force Microscopy (AFM). Surface films of the star copolymers were transferred onto freshly cleaved mica at various pressures. The desired surface pressure was attained by a continuous compression of 0.5 mN m^{-1} at rates of 10 mm min^{-1}. Once the film had equilibrated at a constant Π for at least 15 min, the mica was then pulled at a rate of 1 mm min^{-1}. The transferred film was dried in a desiccator for 24 h and subsequently scanned in tapping mode with a Nanoscope III AFM (Digital Instruments, Inc. Santa Barbara, CA) using silicon probes (Nanosensor dimensions: T = 3.8−4.5 mm, W = 27.6−29.2 mm, L = 131 mm). Using Digital Instruments software, the images were processed with a second-order flattening routine while size, height, and number of domains were measured through section analysis.

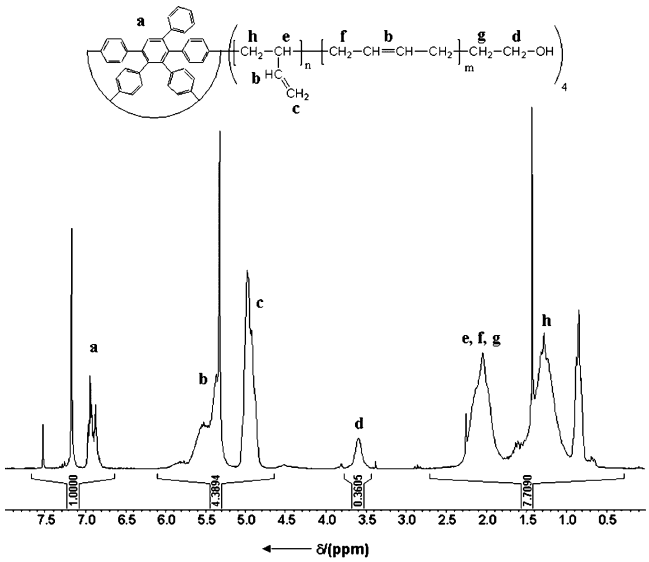

Figure 3. ^{1}H NMR spectra (CD_2Cl_2, 400 MHz) of $(PB\text{-}OH)_4$ hydroxyl ended star polymers ($M_{w,DLS}$ = 1800 g mol^{-1}; M_w/M_n = 1.1).

Polymerization and End-Capping of Butadiene. In a flamed and vacuum-dried three-neck flask, 50.1 mg (6.47×10^{-5} mol) of tetrabromo-initiator was freeze-dried. 12.2 mL of benzene was added to make a precursor solution concentration of 5.3×10^{-2} mol L^{-1}, followed by 0.122 mL (1.55×10^{-3} mol) of 2-methoxyethanol. 1.6 mL (2.07×10^{-3} mol) of *sec*-butyllithium at a concentration of 1.3 M was added to the solution. After 20 min of reaction, butadiene was added. The polymerization was allowed to proceed for 24 h, and then end-capping was accomplished by addition of a large excess of ethylene oxide. The reaction was deactivated by degassed acidic methanol (3 mL of concentrated HCl in 50 mL of methanol). The reaction mixture was concentrated on a rotary evaporator. The LiCl inorganic salts were removed by extraction of a dichloromethane solution of the star polymer with distilled water. The polymer solution was dried over sodium sulfate and concentrated. The star polymer was finally precipitated using methanol to give 1.04 g of a crude product (98%). M_w (SEC/DLS in THF) = 16 400 g/mol; M_w/M_n = 1.05. ^{1}H NMR (CD_2Cl_2): 8.0−6.9 (m, 15H, aromatic resonances from the trifunctional initiator), 7.6−6.7 (m, 22H, aromatic resonances from tetrafunctional initiator), 5.4 (m, 3H, $CH_2-CH{=}CH-CH_2-$ and $CH_2{=}CH-CH-$), 4.9 (s, 2H, $CH_2{=}CH-CH-$), 3.6 (s, 6H

Table 1. Characteristics of Hydroxyl-Functionalized $(PB\text{-}OH)_4$ Star Polymers and $(PB\text{-}b\text{-}PEO)_4$ Amphiphilic Star Block Copolymers

	(PB-OH) star precursor						amphiphilic (PB-*b*-PEO) star copolymer				
stars	M_n[a] (g/mol)	M_w[b] (g/mol)	M_w/M_n[b]	M_n[d] (g/mol)	$M_{n,th}$[c] (g/mol)	% 1,2-PB[d]	M_n[a] (g/mol)	$M_{n,est}$[d] (g/mol)	$M_{n,th}$[e] (g/mol)	M_w/M_n[a]	code
$(PB{-}OH)_3$	1500	2400	1.1	2600	3000	70					
$(PB{-}OH)_3$	25100	32500	1.03	31000	33000	76					
$(PB{-}OH)_4$	800	1800	1.1	1900	1500	64					
$(PB{-}OH)_4$	9400	16400	1.05	15000	17000	64	28300	26200	27000	1.23	$(PB_{76}\text{-}b\text{-}PEO_{57})_4$
$(PB{-}OH)_4$	9400	16400	1.05	15000	17000	64	29400	40600	41500	1.32	$(PB_{76}\text{-}b\text{-}PEO_{137})_4$
$(PB{-}OH)_4$	9400	16400	1.05	15000	17000	64	34500	94600	96000	1.22	$(PB_{76}\text{-}b\text{-}PEO_{444})_4$
$(PB{-}OH)_4$	9400	16400	1.05	15000	17000	64	45800	320000	318000	1.19	$(PB_{76}\text{-}b\text{-}PEO_{1725})_4$

[a] Apparent molar masses determined by SEC in THF using a polystyrene calibration. [b] Determined by SEC in THF equipped with a multiangle light scattering detector. The dn/dc value was measured in THF (dn/dc = 0.094 cm^3/g). [c] $M_{n,th} = M_{Butadiene} \times$ ([butadiene]/[−PhLi]) × n (n = 3 or 4). [d] Estimated by ^{1}H NMR analysis. [e] $M_{n,th} = M_{EO} \times$ ([EO]/[(PB-OH)$_4$] + $M_{w,(PB-OH)_4}$.

Scheme 2. Synthesis of Hydroxyl-Functionalized Star-Shaped Polybutadienes

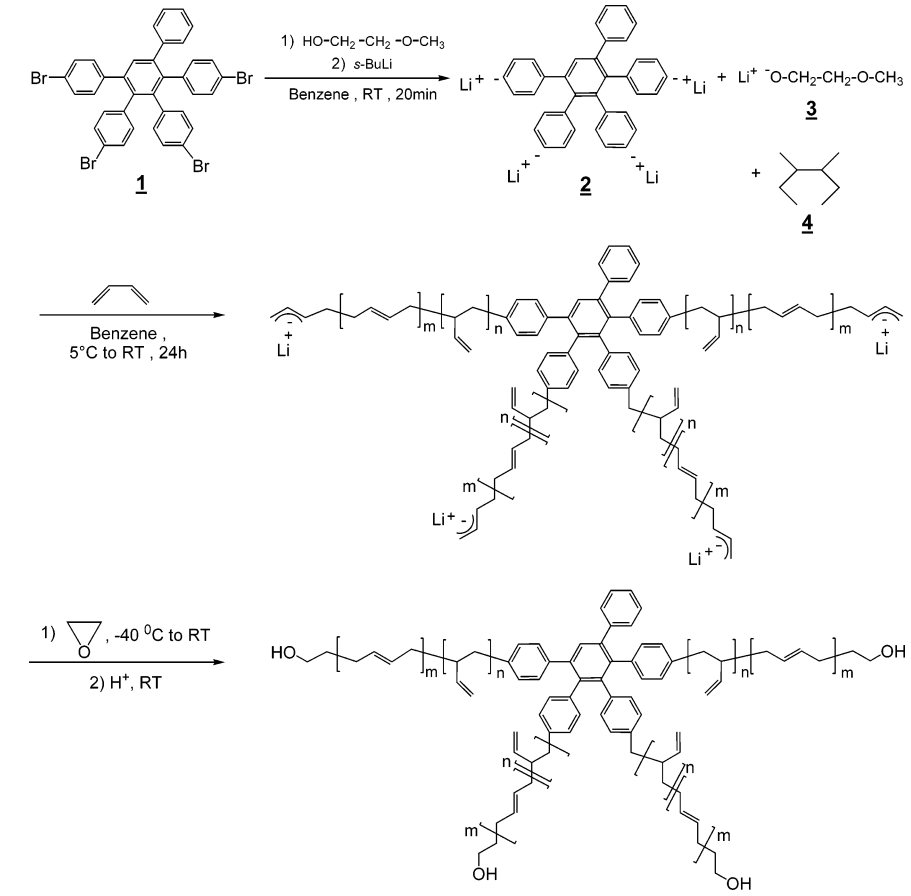

Scheme 3. Synthesis of (PB-*b*-PEO)$_4$ Star Block Copolymers

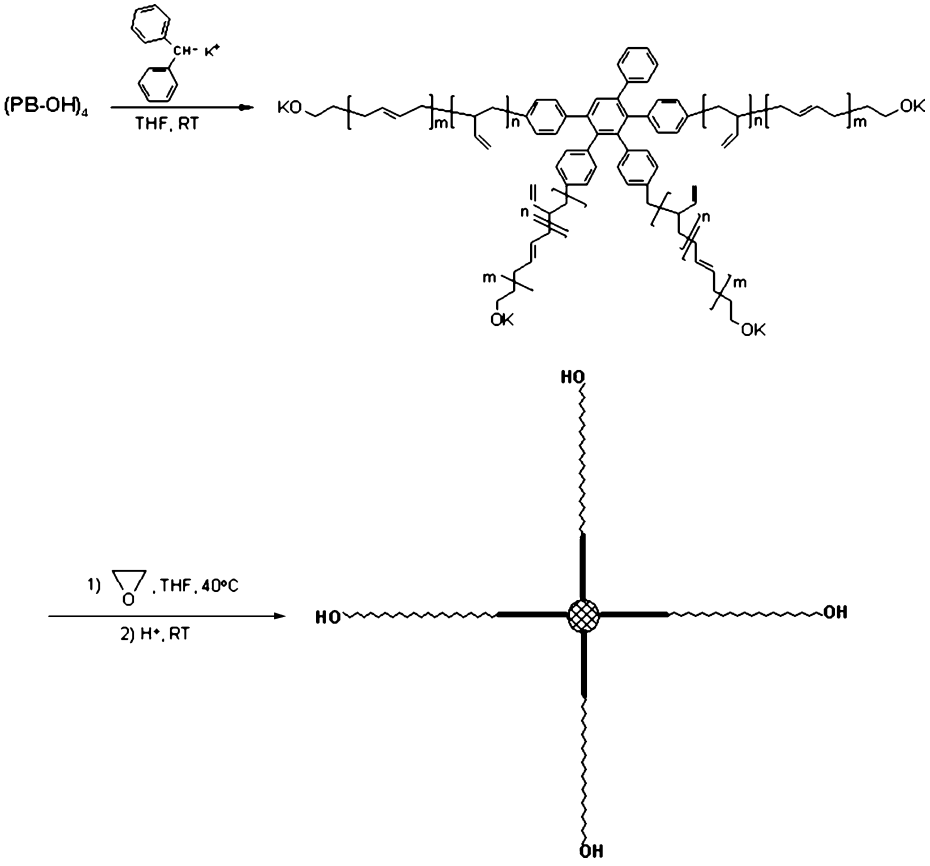

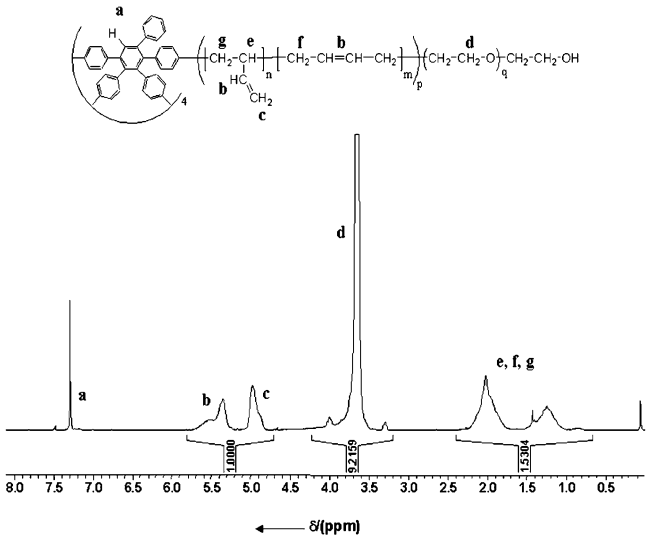

Figure 4. ^{1}H NMR spectra ($CDCl_3$, 400 MHz) of a star copolymer $(PB_{76}\text{-}b\text{-}PEO_{444})_4$ ($M_{n,^1H\ NMR}$ = 94 600 g mol^{-1}; M_w/M_n = 1.22).

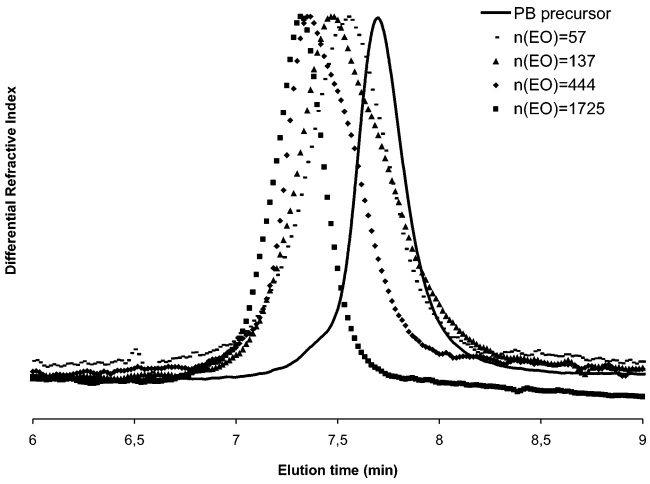

Figure 5. SEC traces of the $(PB\text{-}OH)_4$ precursor ($M_{w,DLS}$ = 16 400 g mol^{-1}; M_w/M_n = 1.05) and of the star copolymers $(PB_{76}\text{-}b\text{-}PEO_n)_4$ (n = 57, 137, 444, and 1725) in THF.

and 8H for the three- and four-armed star, $-CH_2-OH$), 2.0 (b, 5H, $CH_2-CH{=}CH-CH_2-$ and $CH_2{=}CH-CH-$), 1.2 (b, $CH_2{=}CH-C(R)H-CH_2-$).

Polymerization of Ethylene Oxide Initiated by a Hydroxyl-Terminated Polybutadiene Star. Using a flamed and vacuum-dried three-neck flask, the $(PB\text{-}OH)_4$ polybutadiene star was freeze-dried in benzene and then dissolved into anhydrous THF. This solution was titrated by a solution of diphenylmethylpotassium in dried THF of known concentration to give the corresponding multioxanionic species as further described in the Discussion section. The latter species was then used as a macroinitiator for the polymerization of ethylene oxide at 45 °C over 48 h. Deactivation of the polymerization was accomplished by addition of degassed acidic methanol (3 mL of concentrated HCl in 50 mL of methanol). In cases with a relatively low molar mass PEO block, a white precipitate (LiCl) was observed. The crude reaction mixture was concentrated, and the solid was redissolved in dichloromethane. This dichloromethane solution was washed repeatedly with distilled water to remove inorganic salts and concentrated on a rotary evaporator. The star copolymers were precipitated using methanol, diethyl ether, or a mixture of the two depending on the length of each block. ^{1}H NMR ($CDCl_3$): 3.6 (s, $-CH_2-CH_2-O-$) and the polybutadiene region is similar to the corresponding hydroxyl-terminated polybutadiene star resonances (see Figures 2 and 3).

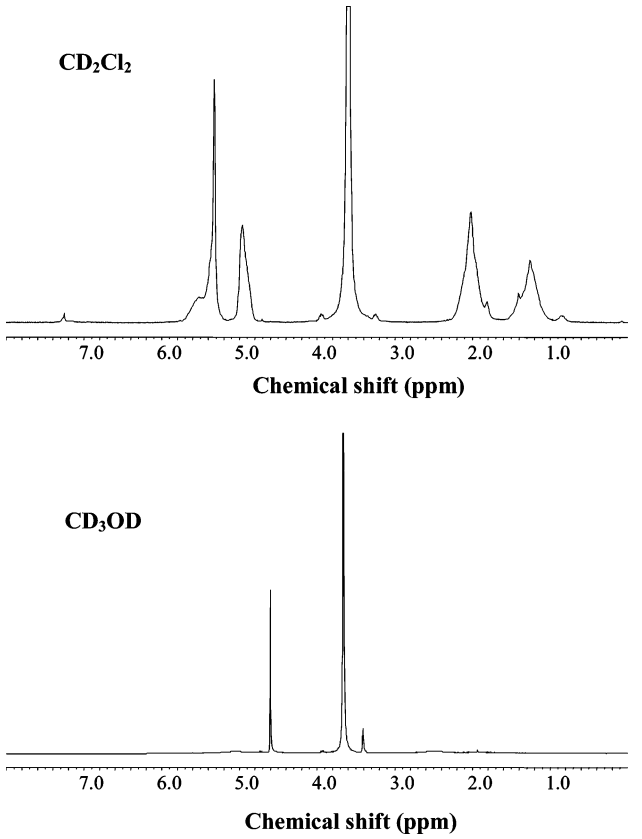

Figure 6. ^{1}H NMR spectra (200 MHz) of $(PB_{76}\text{-}b\text{-}PEO_{444})_4$ in CD_2Cl_2 and in CD_3OD.

3. Results and Discussion

3.1. Synthesis of Amphiphilic Star Block Copolymers. Recently, we described the synthesis of a new category of tri- and tetracarbanionic initiators by the halogen−lithium exchange reaction between a tri- or tetrabromocompound and *sec*-butyllithium.[36] These multicarbanionic initiators were first used for the anionic polymerization of styrene and butadiene to result in well-defined tri- and tetraarmed polystyrene and polybutadiene stars exhibiting monomodal and narrow molar mass distribution. The good efficiency of these multicarbanionic initiators encouraged us to employ them for the preparation of poly(styrene-*b*-butadiene-*b*-methyl methacrylate) ternary star block copolymers.[36] A good agreement between the theoretical and experimental molar masses of each block demonstrated the good definition of these star copolymer structures. The tetracarbanionic initiator was employed here to obtain $(PB\text{-}b\text{-}PEO)_4$ amphiphilic diblock star copolymers.

Synthesis of Star-Shaped Polybutadiene Precursors. The first step of the procedure is the synthesis of the tri- and tetracarbanionic initiators based on the halogen−lithium exchange reaction. As described previously,[41−45] the tetrabromo compound (**1**) is modified to give the corresponding tetraalkyllithium agent (**2**), and importantly for this synthesis, lithium 2-methoxyethoxide (**3**) was utilized to solubilize the polyalkyllithium species due to the σ/μ complex formed between the lithiated species (**2** and **3**).[46] These complexes give stable species and enough steric bulk to prevent aggregation of the polylithiated initiators. Minor amounts of the side product 2-bromobutane, which could deactivate "living" carbanionic sites, were neutralized by a small excess of *sec*-butyllithium yielding 3,4-dimethylhexane (**4**) as an

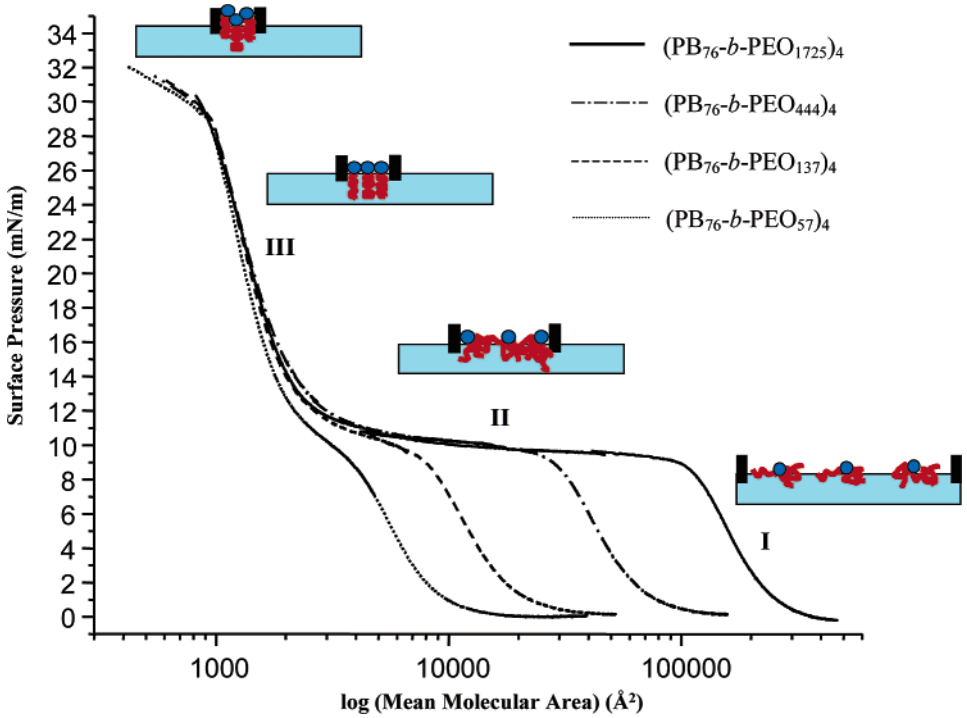

Figure 7. Surface pressure−area per polymer molecule isotherms at 298 K for $(PB_{76}\text{-}b\text{-}PEO_n)_4$ star block copolymers (n = 57, 137, 444, and 1725).

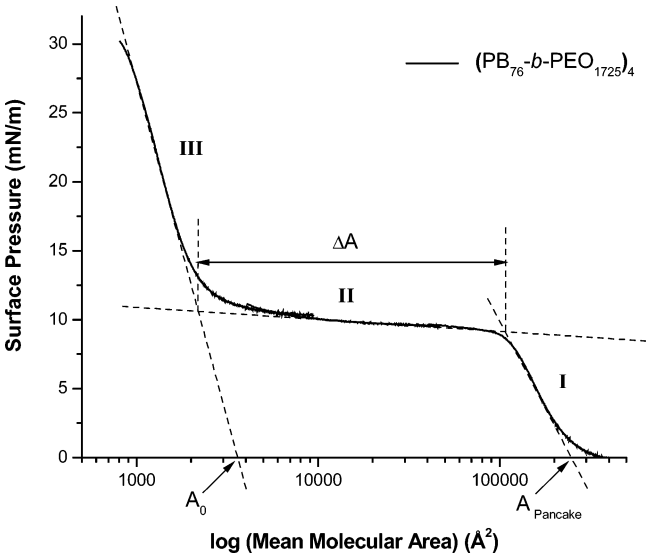

Figure 8. Isotherm of $(PB_{76}\text{-}b\text{-}PEO_{1725})_4$ depicting how measurements of molecular area for the three principal regions are obtained.

inert byproduct. The anionic polymerization of butadiene was carried out in benzene at room temperature using the solubilized tri- and tetralithiated initiator complexes at a concentration of 5.3×10^{-2} M. The polymerization was allowed to proceed for 24 h to ensure complete conversion of monomer, and then end capping was accomplished by adding a large excess of ethylene oxide. During this step, only one $-CH_2CH_2O-$ unit was incorporated as a result of reaction with the chain end lithium counterion. The polybutadienyllithium sites were deactivated by addition of acidic methanol (MeOH/HCl). The resulting inorganic salts are removed by extraction of a dichloromethane solution of the polymer with distilled water.

Different hydroxyl chain ended polybutadiene stars were prepared, and their characteristics are listed in Table 1. The characterization of all the samples by size exclusion chromatography (SEC) showed the disappearance of the peak at low molar mass region, implying total consumption of the tetrafunctional initiator by butadiene polymerization (Figure 1).

The actual molar masses of the hydroxyl chain end polybutadiene stars were determined by SEC/DLS. The molar mass values given by the classical SEC technique were systematically lower than the SEC/DLS values. This underestimation of the molar masses by classical SEC is in agreement with the compact nature of the branched polybutadiene architecture. The calculation of the sample molar mass from ^{1}H NMR data gives an excellent match with those generated from DLS. Even though the polymerization of butadiene was carried out in an apolar solvent such as benzene at room temperature, the microstructure of the resulting PB stars determined by ^{1}H NMR spectroscopy was essentially constituted of a majority of 1,2 repeat units (76% and 64% for the three- and four-armed stars, repectively) (Table 1). This microstructure is the result of the presence of a σ/μ ligand lithium 2-methoxyethoxide, which is an additive polar enough to separate the lithium counterion from the carbanionic chain end and favor 1,2-addition of monomer. The tri- and tetrafunctionalities of the resulting polybutadiene stars were then demonstrated by ^{1}H NMR spectroscopy analysis of star samples with low degrees of polymerization for each arm (Figures 2 and 3). Specifically, the experimental functionality values calculated by the ratios of resonance signals at δ = 6.8−8.0 ppm (aromatic protons of the tri- and tetrafunctional initiators) with those at δ = 3.6 ppm ($-CH_2-$OH chain end protons) are always close to 3 and 4 for the three- and four-armed stars, respectively.

Overall, the polymerization resulted in well-defined star polymers having narrow polydispersity (M_w/M_n < 1.1), molar masses in agreement with calculated values, and a good control of the tri- and tetrafunctional

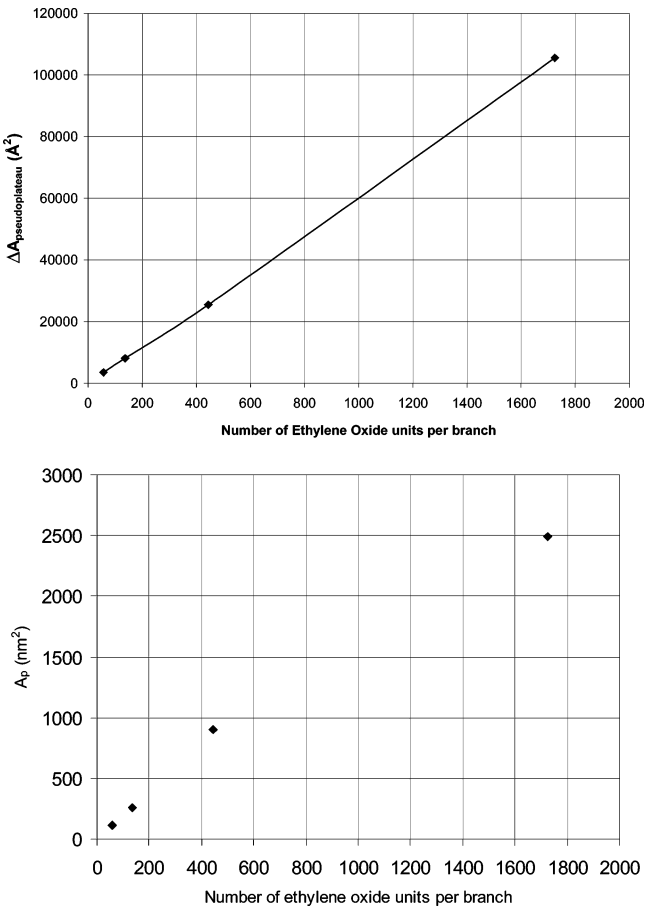

Figure 9. Linear dependence of $\Delta A_{pseudoplateau}$ and A_p on the number of ethylene oxide units per branch.

structures as expected for "living" anionic processes (Table 1). The good definition of these $(PB\text{-}OH)_n$ ($n = 3$ or 4) hydroxyl chain end polybutadiene stars allowed us to use these materials as macroinitiators for the polymerization of ethylene oxide.

Polymerization of Ethylene Oxide by a (PB-OH)$_4$ Macroinitiator. The preparation of (PB-*b*-PEO)$_4$ star block copolymers begins with the transformation of the hydroxyl end groups in the (PB-OH)$_4$ star polymers. The polybutadiene stars were first purified by freeze-drying in benzene or dioxane and then reacted. A solution of diphenylmethylpotassium (DPMK) in THF of known concentration was then added dropwise over a colorless solution of a known amount of (PB-OH)$_4$ in anhydrous THF to titrate the hydroxyl end groups. At stoichiometry, a color change of the solution depending on the initiator concentrations is observed. The macroinitiator solutions are green, red, or yellow for initiator concentrations of 1.5×10^{-3}, 6.25×10^{-4}, or 3.15×10^{-4} M, respectively. In addition, the amount of (PB-OH)$_4$ macroinitiator, calculated from the molecular weight and the mass of polybutadiene stars introduced in the flask, was used to confirm such titrations with DPMK were quantitative. After titration, ethylene oxide was added to the $(PB{-}O{-}K^+)_4$ macroinitiator solution as a liquid at −30 °C, and the solution immediately became colorless. Then the reaction mixture was heated to 45 °C, and the polymerizations were typically run for 3 days to ensure complete conversion of ethylene oxide. Deactivation of the "living" chains was accomplished by the addition of acidic methanol (MeOH/HCl). Potassium chloride salts (KCl) precipitated upon termination were isolated from the hydroxyl-terminated star block copolymers by filtration. After concentration of the (PB-*b*-PEO)$_4$ solution on the rotary evaporator, the block copolymers were precipitated in MeOH for the short PEO blocks and in ethylic ether for the long PEO blocks and finally dried under dynamic vacuum.

All the data for the (PB-*b*-PEO)$_4$ star block copolymers are summarized in Table 1. The recovered polymers were weighed, and the high yields demonstrate that the conversion of ethylene oxide was near quantitative in all cases. Knowing the molar mass of the PB core estimated by SEC/DLS, the actual molar masses of the star block copolymer has been determined by comparing the resonance signal at $\delta = 3.6$ ppm ($(OCH_2CH_2)_n$ (PEO block)) with that at $\delta = 4.8{-}6.0$ ppm (protons of the double bonds (PB block)) (Figure 4). A good agreement was found between the theoretical and experimental molar masses as shown in Table 1.

The apparent molar mass values and polydispersity indices for the (PB-*b*-PEO)$_4$ block copolymers were measured by SEC in THF (Figure 5). A shift to high molar masses with the disappearance of the (PB-OH)$_4$ precursor peak (see (PB_{76}-*b*-$PEO_{1725})_4$), a good control over the PEO molar masses, and the relatively narrow polydispersities ($M_w/M_n < 1.32$) indicate that the block copolymers obtained are free of any PB-OH star precursor, demonstrating that all hydroxyl groups of the (PB-OH)$_4$ star polymer were deprotonated during the deprotonation step and that the alkoxides formed initiated the polymerization of ethylene oxide. The broadening of the molar mass distribution after the EO polymerization merely results for the fact that some alkoxides have a tendency to form aggregates in equilibrium with unaggregated alkoxides. However, it can be seen that as the PEO molar mass per arm in (PB_{76}-*b*-$PEO_{444})_4$ and (PB_{76}-*b*-$PEO_{1725})_4$ increases molar mass distribution narrows with a symmetrical SEC trace for the (PB_{76}-*b*-$PEO_{1725})_4$ sample. In addition, we did not detect any amount of PEO linear homopolymer (which could result from a slight excess of DPMK in the reaction mixture) even in the case of the samples with longest PEO blocks ((PB_{76}-*b*-$PEO_{444})_4$ and (PB_{76}-*b*-$PEO_{1725})_4$): they were indeed precipitated in diethyl ether, and we never observed the presence of linear PEO which would have been totally insoluble in diethyl ether as well.

The amphiphilic character of the (PB-*b*-PEO)$_4$ star block copolymers was first demonstrated by ^{1}H NMR spectroscopy in CD_2Cl_2 and CD_3OD (Figure 6). Figure 6A shows the resonance signals of both the hydrophobic and hydrophilic blocks in solution in CD_2Cl_2, whereas Figure 6B shows that only the resonance signals corresponding to the PEO hydrophilic block are observed in CD_3OD solution. The latter observation is consistent with previous literature results that demonstrate CD_3OD is a good solvent for PEO blocks and a nonsolvent for PB blocks and as a consequence the formation of amphiphilic micelles in CD_3OD with the PB core hidden by the PEO branches.[47−49]

3.2. Behavior at the Air/Water Interface. *Surface Pressure−Area Isotherms.* Surface property characterization of the four different (PB-*b*-PEO)$_4$ star block copolymers started with isotherm measurements. Figure 7 shows the surface pressure−area (π−A) isotherms (25 °C) on compression with a log scale on the x-axis for convenient visualization. The isotherm of each copolymer was reproducible and independent of spreading solution concentration. Together, the isotherms revealed several characteristics. First, all the monolay-

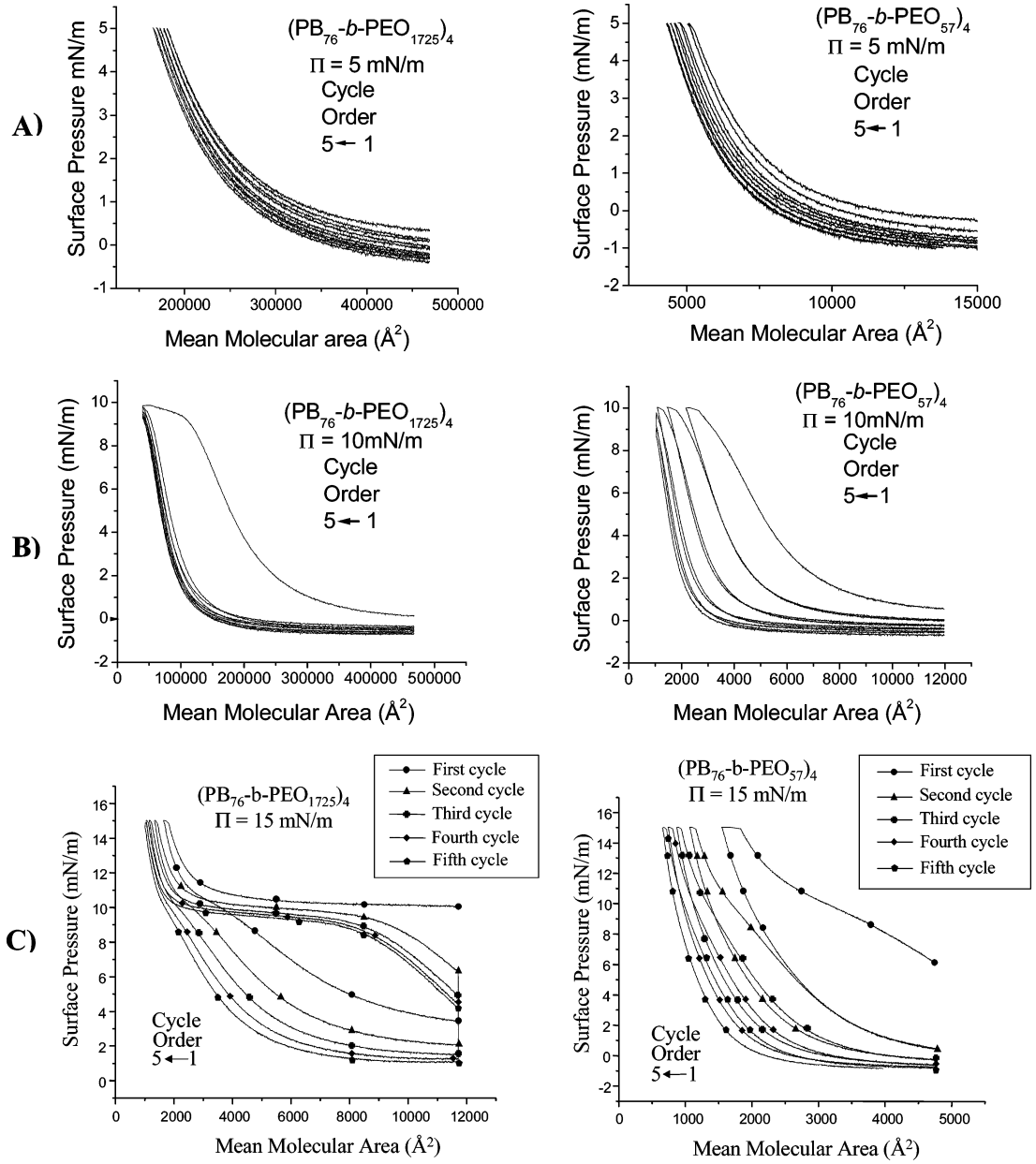

Figure 10. Compression/expansion curves for two different samples of PB_4-*b*-PEO_4 star block copolymers ($(PB_{76}$-*b*-$PEO_{57})_4$ and $(PB_{76}$-*b*-$PEO_{57})_4$) at (A) 5, (B) 10, and (C) 15 mN m^{-1}.

Table 2. Measurements Obtained from Isotherm Experiments of (PB-*b*-PEO)$_4$ Amphiphilic Star Block Copolymers

sample	A_0/molecule (nm^2)	A_0/PB unit (nm^2)	A_0/no. of PB branches (nm^2)	$\Delta A_{pseudoplateau}$ (nm^2)	$A_{pancake}$ (nm^2)
$(PB_{76}$-*b*-$PEO_{57})_4$	29.6	0.097	7.4	35.23	109.77
$(PB_{76}$-*b*-$PEO_{137})_4$	32.66	0.107	8.16	81.22	254.38
$(PB_{76}$-*b*-$PEO_{444})_4$	37.2	0.122	9.3	254.33	904.87
$(PB_{76}$-*b*-$PEO_{1725})_4$	36.01	0.118	9	1055.07	2489.23

ers were compressible up to surface pressures beyond 30 mN m^{-1}. Second, all of the isotherms are characterized by the three distinct regions illustrated in the cartoons of Figure 7: at high molecular areas the so-called "pancake" region (I), a pseudoplateau (II), and the brush region (III) at low surface areas. The dotted lines in Figure 8 also shows the extrapolation used to estimate the three corresponding parameters $A_{pancake}$, A_0, and ΔA. Third, the pressure of the pseudoplateau region was very similar for all samples, while its width varied systematically. In fact, at the highest PEO composition, the pseudoplateau represents more than a 50-fold compression. Fourth, the copolymers (constituted from the same PB core and different PEO chain lengths) occupied similar areas in the high-pressure brush region, independent of the PEO chain length.

Considering the affinity of PEO for the air/water interface and the hydrophobicity of PB, we suppose that the expanded surface film at large molecular areas (I) corresponds to a film dominated by the behavior of PEO at the surface. A quantitative comparison of $A_{pancake}$, the area occupied by the pancakelike PEO domains when adsorbed at the air/water interface, supports this interpretation. A fit of the data revealed a linear dependence of $A_{pancake}$ with the number of EO units ($y = 1.399x + 113.09$; $R^2 = 0.989$), indicating that the "pancake" region area was largely dependent on the PEO block length (Figure 9, bottom).

A)

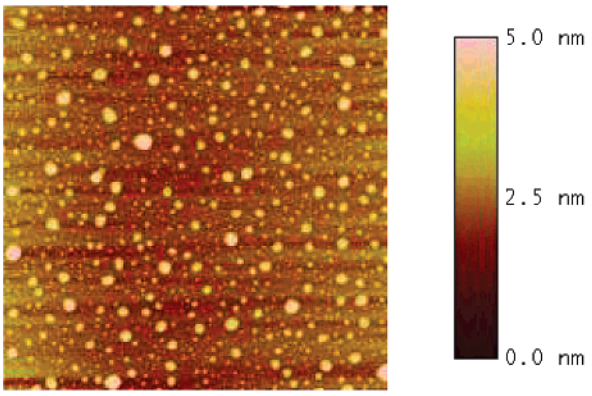

Π=2mN/m

B)

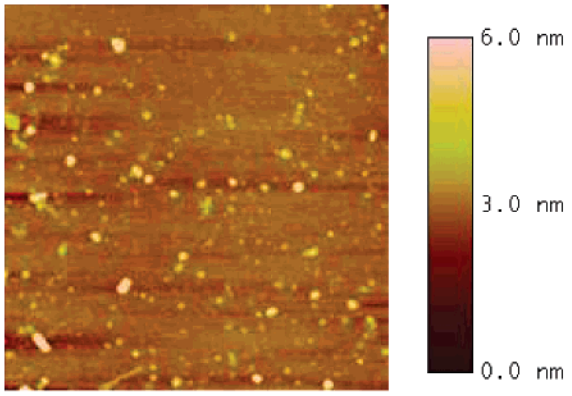

Π=4mN/m

C)

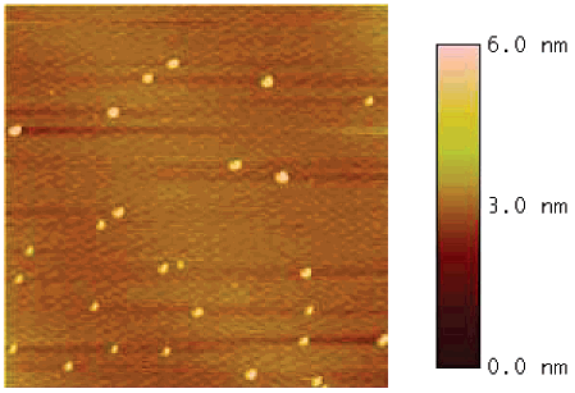

Π=6mN/m

D)

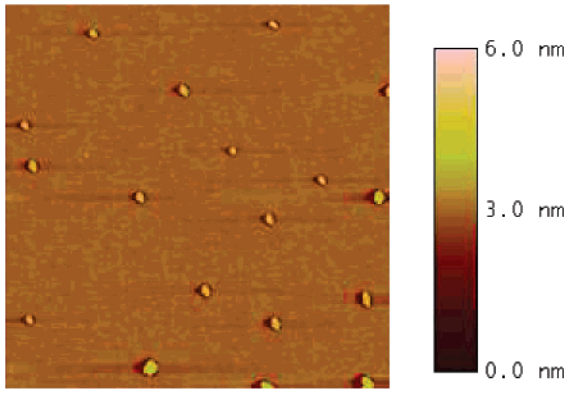

Π=8mN/m

E)

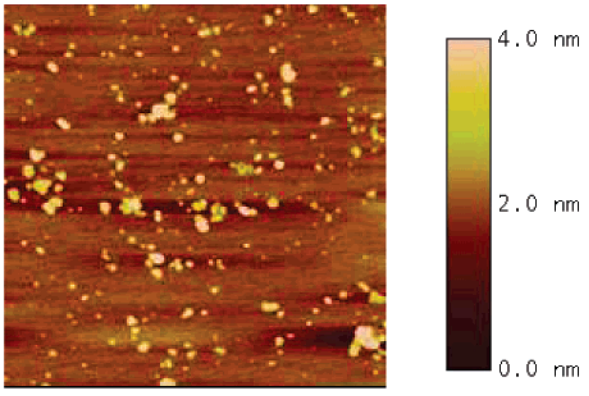

Π=9mN/m

F)

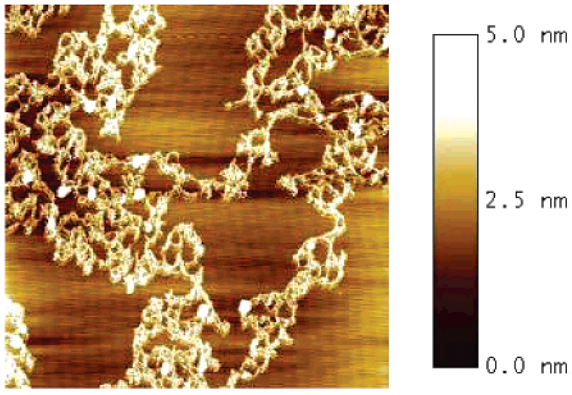

Π=10mN/m

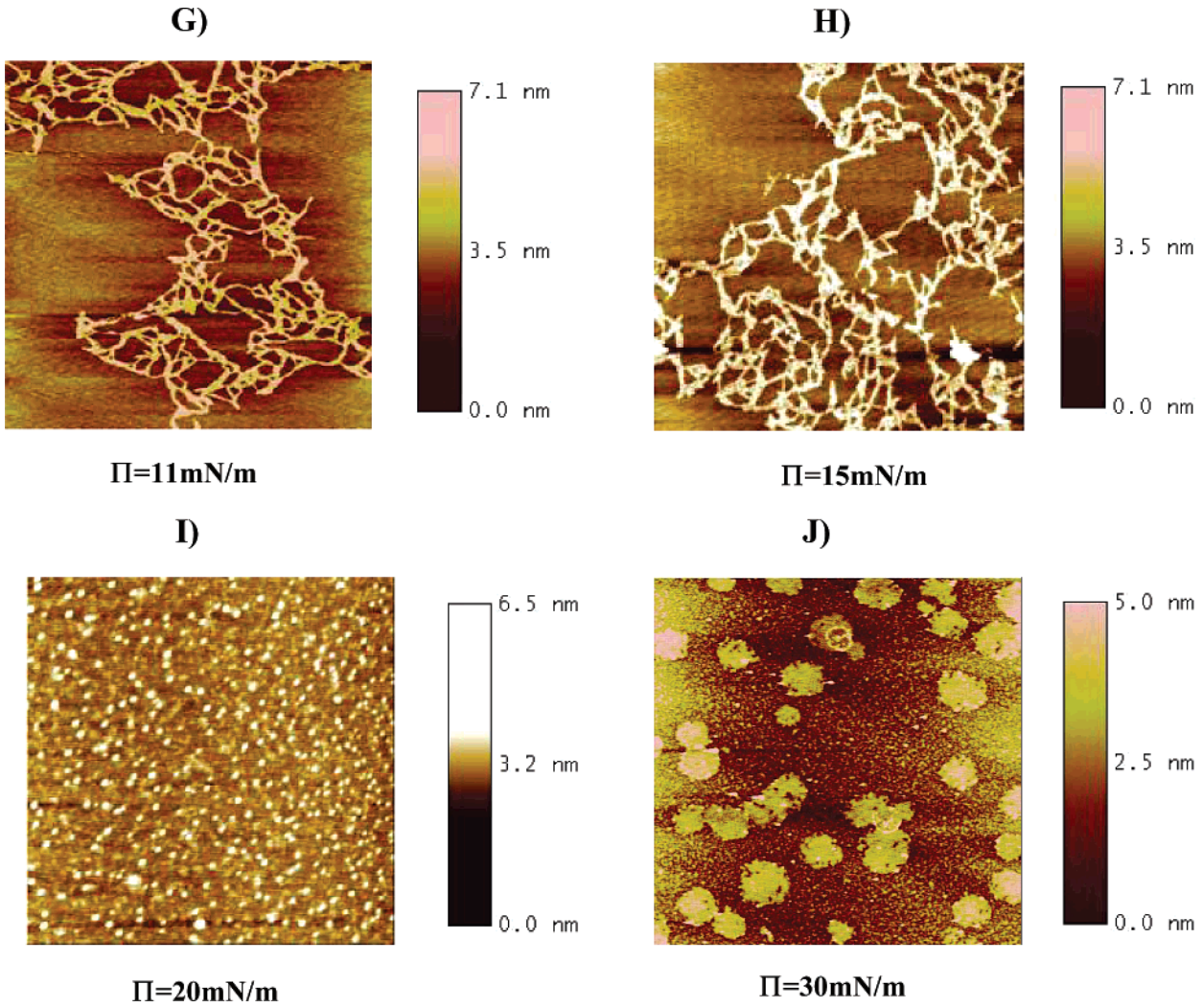

Figure 11. AFM tapping mode amplitude images of the $(PB_{76}$-*b*-$PEO_{1725})_4$ (A, B, C, D, E, F, G, and H) and $(PB_{76}$-*b*-$PEO_{57})_4$ (I and J) star block copolymers transferred to a mica plate support at various surface pressures. The films are scanned at a scan rate of 1 Hz with a scale of 2 × 2 μm (A, B, C, D, E, and I) and 5 × 5 μm (F, G, H, and J).

Second, as the monolayer is compressed, a pseudoplateau is observed at a pressure of about 10 mN m^{-1}, which is a signature of adsorbed EO monomer units at the air−water interface.[50,51] The length of the PEO block clearly influences the length of the pseudoplateau (ΔA) as seen in Figure 7. In fact, a fit of ΔA with the number of EO units gives the very good linear dependence ($y = 0.6136x - 6.0107$; $R^2 = 0.999$) shown at the top of Figure 9. The magnitude of the slope, 61 Å^2/EO repeat unit, is reasonable for PEO units lying flat at the interface. The observed linearity and small intercept implies that the change in area between $A_{pancake}$ and A_0 can be interpreted by PEO segments being successively submerged into the water subphase during compression at ~10 mN/m along the pseudoplateau. This is also in qualitative agreement with previous studies on analogous PS-*b*-PEO star block copolymers at the air/water interface.[18]

Upon further compression, a second large pressure increase is observed up to values of 32 mN m^{-1}, a trend also observed in the case of PB-*b*-PEO linear block copolymers.[27,28] In this regime of high density, a brush conformation is expected. The latter is supported by the theoretical area A_0 that a compact film would occupy at zero pressure. Table 2 reveals that the occupied surface area A_0 is effectively the same for all the four samples (A_0/molecule = 32 ±4 nm^2). The low area per butadiene repeat unit is a strong indication that the PB units have been compressed into a 3D structure rather than lying flat at the air/water interface. This result also confirms that only the PB segments have an effect on the brush region since the copolymers synthesized all possess the same PB core size.

Film Relaxation. By hysteresis experiments, we then investigated the ability of these four arm (PB-*b*-PEO) stars to relax to the same area as that occupied in their original uncompressed state. We examined the effects of pressure variation, compression/expansion cycles, and the PEO block length on the degree of hysteresis, and these results are shown in Figure 10.

Pressure Variation. As shown in Figure 10A, at low pressures ($\Pi < 8$ mN m^{-1}), only minimal hysteresis was observed on compression and expansion, indicating that the surface films were capable of expanding at the same rate as they were compressed independent of the PEO block length. Thus, the star copolymers are elastic and highly surface active in the low-pressure region I.

For pressures in the range of 10 mN m^{-1} a dramatic increase in hysteresis was observed with increasing pressure as shown in Figure 10B,C. This trend is consistent with the interpretation that a higher surface pressure ($\Pi \geq 10$ mN m^{-1}) is necessary to start to submerge the higher MW PEO branches into the water subphase. The observed compression/expansion curves

Table 3. Characteristics of LB Film Experiments

polymer	run	surface pressure (mN/m)	mean molecular area (Mma) (Å^2)	transfer ratio[a]
$(PB_{76}$-*b*-$PEO_{1725})_4$	A	2	217038	1.029
	B	4	173599	1.06
	C	6	146140	0.943
	D	8	119154	1.05
	E	9	96736	2.089
	F	10	10843	1.937
	G	11	3749	2.12
	H	15	1991	1.916
$(PB_{76}$-*b*-$PEO_{57})_4$	F	20	1169	1.84
	G	30	749	1.66

run

[a] (Area of the surface film)/(area of the pulled mica substrate).

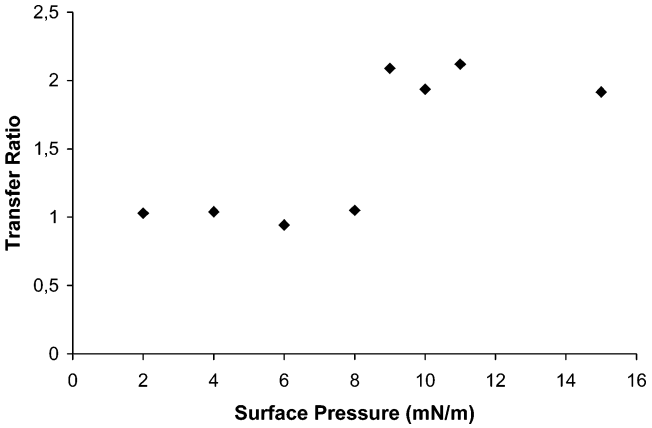

Figure 12. Evolution of transfer ratio with the surface pressure in the case of $(PB_{76}$-*b*-$PEO_{1725})_4$ star block copolymer sample.

also indicate that the surface film now relaxes at a slower rate than the compression.

Compression/Expansion Cycles. Hysteresis also changed with repeated compression/expansion cycles. At lower pressures ($\Pi < 8$ mN m^{-1}), the hysteresis remained relatively minor and independent of the number of compression−expansion cycles applied. In contrast, at higher pressures, the degree of hysteresis, the width of the pseudoplateau, and the pancake limiting area systematically changed. The large initial hysteresis in the left part of Figure 10B may indicate reorganization of the high-MW PEO arms between the first and second compression. Subsequent creep to smaller surface areas indicates that with each cycle slightly more PEO is submerged into the water subphase and does not resurface over the time of the experiment. The large hysteresis loop observed at higher pressures ($\Pi > 10$ mN m^{-1}) for samples consisting of very long PEO chains

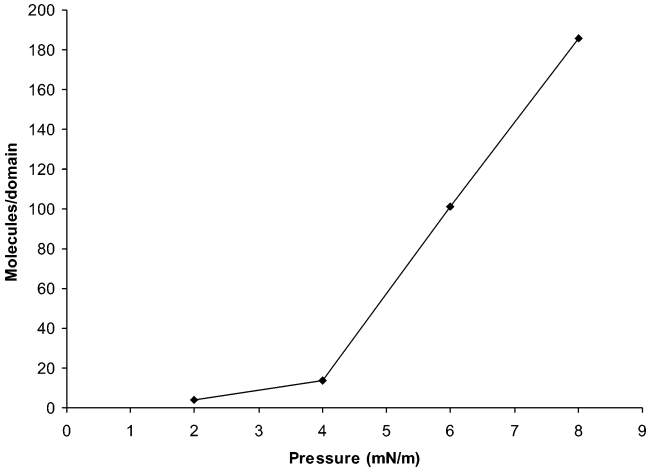

Figure 13. Dependence of the number of molecules per domain on the surface pressure in thecase of the $(PB_{76}$-*b*-$PEO_{1725})_4$ star block copolymer sample. The general trend shows that as pressure increases, more molecules aggregate (dramatic increase from $\Pi = 4$ mN/m) to form the observed circular PB microdomains.

($(PB_{76}$-*b*-$PEO_{1725})_4$; Figure 10C, left) indicates that the film has considerable viscoelastic character, possibly due to entanglement of the submerged PEO segments. Ongoing experiments with a broader range of samples should provide additional insight into the observed hysteresis behavior.

AFM Characterization of the Transferred Monolayers. Atomic force microscopy was used to study the morphology of surface films at the air/water interface after transfer to a solid surface. To this end, Langmuir−Blodgett films of two different samples $(PB_{76}$-*b*-$PEO_{1725})_4$ and $(PB_{76}$-*b*-$PEO_{57})_4$ were transferred to mica substrates over a range of pressures. Table 3 and Figure 12 shows that for applied surface pressures below 9 mN/m positive transfer ratio values of ~1.0 were observed, indicating "ideal" transfer with no change in macroscopic film dimensions, whereas surface pressures above 8 mN/m lead to transfer ratios of ~2.0 or significant densification of the surface film upon transfer. In all cases LB transfers were characterized by a linear instantaneous transfer ratio, indicating that the monolayer was transferred uniformly over the entire mica substrate.

Because of the hydrophilic nature of the mica, we assume PEO transfers as the bottom layer, represented in the scanned images as the continuous dark phase, whereas PB occupies the top portion of the film corresponding to the white higher elevation microdomains shown in Figure 11.

Table 4. AFM Characteristics of (PB-*b*-PEO)$_4$ Four-Arm Star Copolymers

run	surface pressure (mN/m)	av diameter of PB domains (nm) (± 7)	vertical height (nm) (±1)	no. of domains (±50)	PB coverage area[a] (%) (±10)	no. of molecules per domain[b] (±10)
A	2	61	2.234	445	32	4
B	4	67	3.413	170	15	14
C	6	71	4.729	27	3	101
D	8	132	4.837	18	6	186
E	9	84	4.526	193	9	22
F	10	*c*	4.9	*c*	*c*	*c*
G	11	*c*	5.09	*c*	*c*	*c*
H	15	*c*	5.181	*c*	*c*	*c*
F	20	54	2.082	380	22	900
G	30	550	5.282	38	36	87836

[a] Coverage area = (πr^2)(number of domains)/scan area. [b] Molecules/domain = scan area/[(number of domains)(mean molecular area)]. [c] At these surface pressures, films are in a multilayer regime.

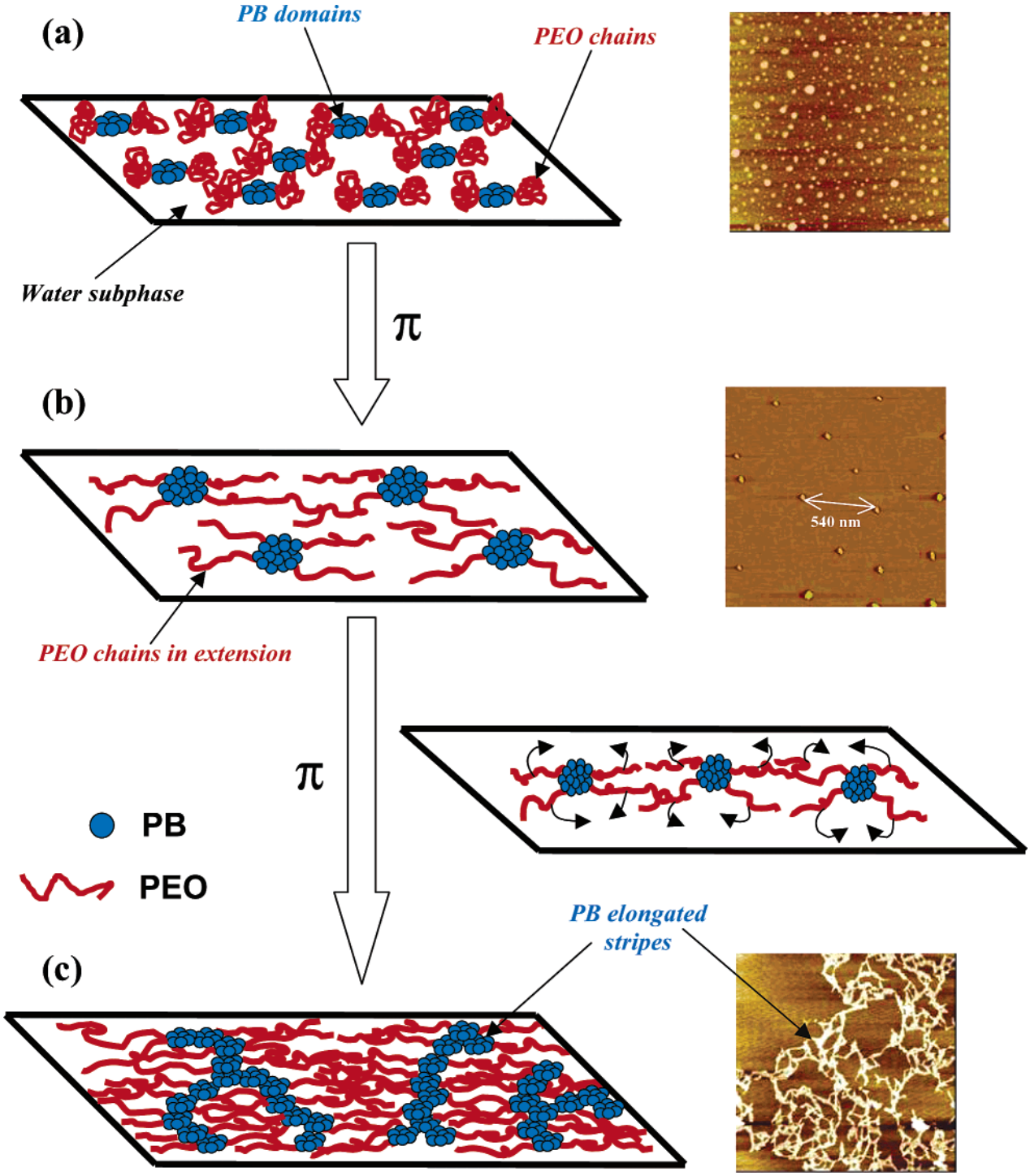

Figure 14. Model proposed to explain the formation of a network of elongated stripes. (a) Long PEO branches staying at the water surface as globules create a weak separation between the PB microdomains. (b) As the surface pressure increases, the PEO blocks are pushed to the maximum hydration by a total extension of their chains on the surface of water. (c) Upon further compression, the PEO chains, to long to be totally submerge into the water subphase, shift to allow the PB microdomains to aggregate through only one point of contact to give elongated stripes.

Effect of Surface Pressure. First, an effect of the surface pressure can be seen (Figure 11) in the "pancake" region for the sample with the longest PEO blocks. At lower pressures (Π = 2 mN m^{-1}) the PB microdomains are not homogeneous in size. However, when increasing pressure from Π = 2 to 8 mN m^{-1}, the PB microdomains are more organized, of larger size, and less numerous for a same area. These observations were confirmed by the quantitative analysis of the AFM scans shown in Table 4. In comparing AFM scans (Figure 11A−D), first a gradual increase in the diameter of PB domains (from 61 to 132 nm), their height (from 2 to 5 nm), and the number of molecules per PB domain (from 4 to 186) and second a decrease in the number of PB domains (from 445 to 18) and in the PB coverage (from 32% to 6%) with the surface pressure increasing were observed (Table 4).

The above trend is also observed in the molecules/domain vs pressure curve of Figure 13, which shows more molecules continually aggregating (dramatic increase above pressure Π = 4 mN/m) to form larger circular 2D micelles. These data are a strong indication

that the surface micelles formed on spreading the PB-*b*-PEO stars are fluid and dynamic at the air/water interface, in sharp contrast to PS-*b*-PEO systems where vitrification of PS leads to frozen surface micelles.

The AFM data also show that the during compression the distance between the PB microdomains increases from an average distance of 70 nm at $\Pi = 2$ mN m^{-1} to 540 nm at $\Pi = 8$ mN m^{-1}. The estimated theoretical length of one extended PEO branch (1725 EO units and assuming 3.19 Å per EO unit) is about 550 nm, which is very close to the average distance between two PB microdomains at $\Pi = 8$ mN m^{-1} (540 nm) illustrated in Figure 14.

At higher pressures ($\Pi > 8$ mN m^{-1}), a second type of morphology is observed (Figure 11E−H). This change in morphology is mirrored by a significant increase of the transfer ratio (TR) illustrated in Figure 12. The sudden jump in TR from 1.0 to 2.0 implies significant densification of the film upon transfer in the pseudoplateau region ($\Pi \geq 8$ mN m^{-1}). The AFM data show that at $\Pi = 9$ mN/m PB microdomains are spaced much more closely compare to $\Pi = 8$ mN/m and then form elongated stripes, or chains, at $\Pi = 10$ mN/m. The onset of the chain morphology correlates with the onset of significant hysteresis (Figure 10C) observed with the PEO_{1725} blocks. Moreover, neither the chain morphology (Figure 11I,J) nor the same hysteresis (Figure 10C) is observed for the shorter PEO_{57} material, indicating a PEO length influence chaining aggregation.

The observed results led to the model shown in Figure 14 for the $(PB_{76}$-*b*-$PEO_{1725})_4$ block copolymer. At low pressure, microdomains of polydisperse size, some 2 nm vertical thickness, and few polymer chains per domain are observed. The relatively low density of PEO chains allows these domains to be closely spaced and the PEO chains to be in a relatively compact conformation. Upon compression, the PB domains clearly flow and coalesce to form progressively larger surface micelles of more monodisperse size and higher and higher PEO chain densities that should lead to an overall extension of the PEO segments. We suppose that reduction in the line tension between the PB and PEO rich phases helps drive the aggregation. This process also increases the vertical thickness and significantly increases the lateral spacing between domains. At higher surface pressure ($\Pi > 8$ mN m^{-1}), and perhaps also associated with compaction during LB transfer, we suppose the PB microdomains start to chain as illustrated in Figure 14C. During chaining we hypothesize that the long PEO chains are further extended in a direction perpendicular to the chain axis and this hinders spherical aggregation and favors aggregate through points of contact at opposite ends of the elongated domain. Similar surface morphology has also been observed in the case of PB-*b*-PEO linear block copolymers.[27] At higher applied surface pressures, we suppose that the remaining PEO chains are hydrated and larger aggregates are formed, quickly leading to thicker films.

In contrast, we suppose that the short PEO branches of the $(PB_{76}$-*b*-$PEO_{57})_4$ material are much more easily submerged into the water subphase at higher pressure, and micelle chaining is hindered.

4. Conclusion

A homologous series of novel $(PB$-*b*-$PEO)_4$ amphiphilic four-arm star block copolymers were prepared that afforded samples of narrow and well-defined molar mass distribution. When spread at the air/water interface, all four star copolymers formed stable and reproducible monolayers. Surface pressure−area isotherms indicated compression-induced hydration of the PEO segments influenced the monolayer behavior at low surface pressures while packing of the PB segments playing a prominent role at higher pressures. Surface relaxation studies demonstrated hysteresis in both the pancake and pseudoplateau regions, with a systematic influence of the PEO content. AFM studies showed characteristic morphology which evolved from two types of separated surface micelles to a chained micelle as the applied surface pressure was varied. Overall, the morphology of PB-*b*-PEO materials varied significantly and systematically during monolayer compression. We suppose that this is in part due to the low T_g and resulting fluidity of the PB segment, compared to analogous PS-*b*-PEO copolymers, or any system where one block can vitrify. Because they can be subsequently cross-linked, these PB-*b*-PEO star copolymers may be interesting for nanopatterning, nanolithography, and related applications.

Acknowledgment. The authors acknowledge financial support from DOE (BES), DST, and the NSF REU program.

References and Notes

(1) Piirma, I. In *Polymeric Surfactants, Surfactant Science Series*; M. Dekker: New York, 1992.
(2) Laschewsky, A. *Adv. Polym. Sci.* **1995**, 1.
(3) Velichkova, R. S.; Christova, D. C. *Prog. Polym. Sci.* **1995**, *20*, 819.
(4) Harris, J. M. *Poly(ethylene glycol) Chemistry. Biotechnical and Biomedical Applications*; Plenum Press: New York, 1992.
(5) Alexandris, P.; Lindman, B. *Amphiphilic Block Copolymers. Self-Assembly and Applications*; Eds.; Elsevier: Amsterdam, 2000.
(6) Bijsterbosch, H. D.; de Haan, V. O.; de Graaf, A. W.; Mellema, M.; Leermarkers, F. A. M.; Cohen Stuart, M. A.; van Well, A. A. *Langmuir* **1995**, *11*, 4467.
(7) Goncalves da Silva, A. M.; Filipe, E. J. M.; d'Oliveira, J. M. R.; Martinho, J. M. G. *Langmuir* **1996**, *12*, 6547.
(8) Goncalves da Silva, A. M.; Simoes Gamboa, A. L.; Martinho, J. M. G. *Langmuir* **1998**, *14*, 5327.
(9) Fauré, M. C.; Basserau, P.; Carignano, M. A.; Szleifer, I.; Gallot, Y.; Andelman, D. *Eur. Phys. J. B* **1998**, *3*, 365.
(10) Fauré, M. C.; Basserau, P.; Lee, L. T.; Menelle, A.; Lheveder, C. *Macromolecules* **1999**, *32*, 8538.
(11) Cox, J. K.; Constantino, B.; Yu, K.; Eisenberg, A.; Lennox, R. B. *Langmuir* **1999**, *15*, 7714.
(12) Cox, J. K.; Yu, K.; Eisenberg, A.; Lennox, R. B. *Phys. Chem. Chem. Phys.* **1999**, *1*, 4417.
(13) Richards, R. W.; Rochford, B. R.; Webster, J. R. P. *Polymer* **1997**, *38*, 1169.
(14) Francis, R.; Skolnik, A. M.; Carino, S. R.; Logan, J. L.; Underhill, R. S.; Angot, S.; Taton, D.; Gnanou, Y.; Duran, R. S. *Macromolecules* **2002**, *35*, 6483.
(15) Gragson, D. E.; Jenson, J. M.; Baker, S. M. *Langmuir* **1999**, *15*, 6127.
(16) Baker, S. M.; Leach, K. A.; Devereaux, C. E.; Gragson, D. E. *Macromolecules* **2000**, *33*, 5342.
(17) Devereaux, C. A.; Baker, S. M. *Macromolecules* **2002**, *35*, 1921.
(18) Logan, J.; Masse, P.; Skolnik, A. M.; Francis, R.; Taton, D.; Duran, R. S.; Gnanou, Y., to be published.
(19) Maskos, M.; Harris, J. R. *Macromol. Rapid Commun.* **2001**, *22*, 271.
(20) Hillmyer, M. A.; Bates, F. S. *Macromolecules* **1996**, *29*, 6994.
(21) Discher, D. E.; Won, Y. Y.; Ege, D. S.; Lee, J. C. M.; Bates, F. S.; Discher, B. M.; Hammer, D. A. *Science* **1999**, *284*, 1143.
(22) Won, Y. Y.; Davis, H. T.; Bates, F. S. *Science* **1999**, *283*, 960.
(23) Liu, G. J.; Qiao, L. J.; Guo, A. *Macromolecules* **1996**, *29*, 5508.
(24) Thurn-Albrecht, T.; Schotter, J.; Kästle, G. A.; Emley, N.; Shibauchi, T.; Krusin-Elbaum, L.; Guarini, K.; Black, C. T.; Tuominen, M. T.; Russell, T. P. *Science* **2000**, *290*, 2126.

(25) Doshi, D. A.; Huesing, N. K.; Lu, M.; Fan, H.; Lu, Y.; Simmons-Potter, K.; Potter, B. G., Jr.; Hurd, A. J.; Brinker, C. J. *Science* **2000**, *290*, 107.
(26) Discher, B. M.; Bermudez, H.; Hammer, D. A.; Discher, D. E.; Won, Y. Y.; Bates, F. S. *J. Phys. Chem. B* **2002**, *106*, 2848.
(27) Ahmed, F.; Hategan, A.; Discher, D. E.; Discher, B. M. *Langmuir* **2003**, *19*, 6505.
(28) Bowers, J.; Zarbakhsh, A.; Webster, J. R. P.; Hutchings, L. R.; Richards, R. W. *Langmuir* **2001**, *17*, 131.
(29) Milling, A. J.; Hutchings, L. R.; Richards, R. W. *Langmuir* **2001**, *17*, 5297.
(30) Hadjichristidis, N., Pispas, S., Floudas, G. A., Eds.; *Block Copolymers: Synthetic Strategies, Physical Properties and Applications.*; John Wiley & Sons: Hoboken, NJ, 2003.
(31) Bates, F. S. *Science* **1991**, *251*, 898.
(32) Xu, J.; Zubarev, E. R. *Angew. Chem., Int. Ed.* **2004**, *43*, 5491.
(33) Quirk, R. P.; Tsai, Y. *Macromolecules* **1998**, *31*, 4372.
(34) Vasilenko, N. G.; Rebrov, E. A.; Muzafarov, A. M.; Eswein, B.; Striegel, B.; Möller, M. *Macromol. Chem. Phys.* **1998**, *199*, 889.
(35) Tsitsilianis, C.; Vogiagis, G.; Kallitsis, J. K. *Macromol. Rapid Commun.* **2000**, *21*, 1130.
(36) Matmour, R.; Lebreton, A.; Tsitsilianis, C.; Kallitsis, I.; Héroguez, V.; Gnanou, Y. *Angew. Chem., Int. Ed.*, in press.
(37) Suffert, J. *J. Org. Chem.* **1989**, *54*, 509.
(38) Francis, R.; Taton, D.; Logan, J. L.; Masse, P.; Gnanou, Y.; Duran, R. S. *Macromolecules* **2003**, *36*, 8253.
(39) Cheng, K. J.; Ding, Z. B.; Wu, S. H. *Synth. Commun.* **1997**, *27*, 11.
(40) Wolfe, J. F.; Arnold, F. E. *Macromolecules* **1981**, *14*, 909.
(41) Trepka, W. J.; Sonnenfeld, R. J. *J. Organomet. Chem.* **1969**, *16*, 317.
(42) Gilman, H.; Gorsich, R. D. *J. Am. Chem. Soc.* **1956**, *78*, 2217.
(43) Jedlicka, B.; Crabtree, H.; Per, E. M. S. *Organometallics* **1997**, *16*, 6021.
(44) Winkler, H. J. S.; Winkler, H. *J. Am. Chem. Soc.* **1966**, *88*, 969.
(45) Applequist, D. E.; O'Brien, D. F. *J. Am. Chem. Soc.* **1963**, *85*, 743.
(46) Bayard, P.; Jérôme, R.; Teyssié, P.; Varshney, S.; Wang, J. S. *Polym. Bull. (Berlin)* **1994**, *32*.
(47) Fréchet, J. M. J.; Gitsov, I. *Macromol. Symp.* **1995**, *98*, 441.
(48) Gitsov, I.; Fréchet, J. M. J. *Macromolecules* **1993**, *26*, 6536.
(49) Gitsov, I.; Fréchet, J. M. J. *J. Am. Chem. Soc.* **1996**, *118*, 3785.
(50) Kawaguchi, M.; Tohyama, M.; Mutoh, Y.; Takahashi, A. *Langmuir* **1988**, *4*, 407.
(51) Henderson, J. A.; Richards, R. W.; Penfold, J.; Thomas, R. K.; Lu, J. R. *Macromolecules* **1993**, *26*, 4591.

MA050578Z